Catalysis Today 181 (2012) 95–101

Contents lists available at ScienceDirect

Catalysis Today

journal homepage: www.elsevier.com/locate/cattod

Nitrogen modified metal oxide surfaces

I. Bertóti*

Chemical Research Center,[1] Hungarian Academy of Sciences, Institute of Materials and Environmental Chemistry, P.O. Box 17, H-1525 Budapest, Hungary

ARTICLE INFO

Article history:
Received 10 March 2011
Received in revised form 2 June 2011
Accepted 21 June 2011
Available online 23 July 2011

Keywords:
Metal oxinitrides
Nitrogen-modified oxides
Ion beam modification
Nitrogen bonding states
Mechanism of oxide–nitride transformation

ABSTRACT

Nanoscale surface modification of a number of metal oxides was performed by bombarding them with N_2^+ of 1–5 keV energy. Compositional and chemical state alterations, the valence state of the metals, the chemical states of the built-in nitrogen, were monitored by quantitative XPS analysis, performed *in situ*, without exposing the modified surface to the environment. It is demonstrated that N_2^+ bombardment created oxygen deficient surface with significantly lower oxygen to metal (O/Me) ratio than that produced by the purely ballistic effect of Ar^+ bombardment of similar energy and ion-dose. This "excess" oxygen-loss, detected at N_2^+ bombardment, is substituted by an equal number of nitrogen atoms in the lattice of the reduced oxide. The implanted nitrogen established chemical bonds predominantly with the metal as manifested by its XPS chemical shift, creating by this a metal oxinitride on the surface of the parent oxide. The observed alterations are interpreted in the light of ion–solid interaction, involving the thermodynamic stability and the valence state of the oxides. A mechanism is proposed to elucidate the observed, thermodynamically unfavoured oxide-to-nitride transformation. The presented results offer a straightforward way for altering the electronic structure of the surface of oxides which may be beneficial for different, especially for photocatalytic applications of the modified oxides.

1. Introduction

Metal oxides are gaining increasing importance in different novel high-tech areas. Beyond the broad conventional, mostly structural applications, more recently their functional application, based on the electronic properties of the outermost surface, are occupying leading position in the research and development of these materials. Exact knowledge of the surface electronic state is of principal importance especially for nano-disperse oxide materials having very large surface-to-bulk atomic ratio. Due to additional specific properties, these latter types of oxides are gaining applications in heterogeneous catalysis, photocatalysis, gas sensing, solar energy conversion, etc. The properties of oxides may be favourably modified for certain applications by altering only their surface composition, oxygen-to-metal stoichiometry, and as a novel approach, replacing oxygen with other elements, modifying by this the electronic structure and other properties.

Minor changes of the electronic structure involving modification of the band-gap and charge carrier mobility may induce significant alteration of the adsorption and activation of molecules from the gas phase, residence time of these species on the surface and energetics of the desorption of the reaction products. Another important aspect is the band-gap dependent photon absorption and the photon–electron conversion and the related photocatalytic activity of the modified surface [1,2].

Partial reduction of oxides, recognized to be a trivial way of modification, is equivalent of creating increasing number of oxygen vacancies in the oxide lattice. Here it is important to point out the principal differences in the stability of such 'partially reduced' states. For the oxides where the metallic constituent has one single preferential valence/oxidation state (e.g. Al_2O_3) there is a high thermodynamic driving force, i.e. a strong tendency to re-establishing the stable fully oxidised state.

For those oxides where the metallic constituent has two or more stable valence states, the build-up of oxygen vacancies in the highest or higher oxide, would 'relax' to a stable lower oxide: e.g. Fe_2O_3 to Fe_3O_4, FeO, or V_2O_5 to V_2O_4, V_2O_3, etc. Similar transformations are broadly recognised in various heterogeneous catalytic and also in gas sensing processes [1–3].

In addition to 'simple' oxides containing one metallic element, 'complex' oxides with two or more cations are also considered as candidates for enhancing performance or optimizing properties for various applications [4,5]. In this respect, distinguished attention has been paid recently to anion-modified oxides, especially to those modified by nitrogen. Examples have been reported on oxides with low N-doping level [1,3], and also on those where a major part of the lattice oxygen is replaced by nitrogen forming bulk-phase oxinitrides [5–10].

From the difference in Pauling's electronegativity (3.50 for O and 3.07 for N) follows that bonding in oxinitrides should be more covalent than in oxides. Consequently, smaller band gaps for oxinitrides

* Tel.: +36 1 438 1156; fax: +36 1 438 1147.
E-mail address: bertoti@chemres.hu
[1] http://www.chemres.hu/aki.

0920-5861/$ – see front matter © 2011 Elsevier B.V. All rights reserved.
doi:10.1016/j.cattod.2011.06.017

can be expected [5,9]. The band gap values published for oxinitrides, falling in the 1.8–3.3 eV range, closely overlapping with the solar spectrum, making this class of materials very attractive for applications such as visible-light driven photocatalysts. In connection with this, tuning of the optical properties is of prime concern. Substantial theoretical and experimental efforts are devoted to the most promising representative, to the $TiO_{2-x}N_x$ phase [1].

Numerous successful attempts of application of oxinitride materials in various catalytic processes have been reported recently. Among these, decomposition of ammonia on ZrON [11,12], decomposition of organic molecules on ZnGaON and ZnGeON [13,14] and on P-containing AlPON or ZrPON catalysts [15,16] are to be mentioned. Visible light activation was successfully applied for water-splitting on TiON [17], ZrON [16], GaON [18], TaON [19] and on other modified complex oxides [4] and also disinfection of water, e.g. by TiON [17] became the subject of intensive research together with different other catalytic processes [20].

Majority of the oxinitride catalysts are prepared by conventional thermally activated thermodynamically feasible processes. As far as the heterogeneous catalytic processes are governed mainly by the electronic structure of the surface of the catalyst, it may be sufficient to create a thin oxinitride layer on the surface of the oxides possessing properties similar to the reported bulk-phase oxinitrides cited above.

It has been recognised for long that bombardment of oxides by energetic particles, e.g. by Ar^+, leads to oxygen loss, i.e. to reduction [21,22]. We have reported earlier [23–26] that the oxygen-deficient state can be conveniently created in a thin, 10–20 nm thick, surface layer by bombarding the oxides not only by Ar^+ but also by N_2^+ ions with energy of the 2–5 keV range. When N_2^+ ion beam is applied nitrogen is incorporated into the host oxide forming an oxinitride surface film. Performing such modification, XPS can be applied as a precise quantitative technique for determining the oxygen loss, the build-up of implanted nitrogen and the valence state of the metal, finally the electronic state of the topmost 5–10 nm layers on the surface of the oxides. Application of this method provides profound insight into the consequences of such modifications especially when the ion-beam treatment is performed in the XP spectrometer and the modified surface is studied *in situ*.

In this work a simple straightforward way of modification of oxide surfaces by energetic nitrogen ions is proposed. Examples on N_2^+ ion beam modification of a number of metal oxides are presented. The electronic structure of the nanoscale oxinitride layers is determined by XPS and compared with those of the parent oxides and the corresponding bulk nitrides. The mechanism of the oxinitride formation is discussed.

2. Experimental

2.1. Samples

The samples were selected as to be reliably representative for the stoichiometric compound with the nominal composition corresponding to the indicated chemical formulae. This is why commercial mirror-polished single crystal slices of Al_2O_3, SiO_2 and TiO_2 were applied after washing and rinsing in standard manner. Freshly cleaved surface of the V_2O_5 single crystal was applied without further treatment. Powdered GeO_2, ZrO_2 and Nb_2O_5 samples were pelleted and treated in oxygen plasma ($\sim 10^{-3}$ mbar) for removing carbon contamination.

2.2. Ion-beam treatment

Ion bombardments were performed using a hot-filament equipped ion gun fed with high-purity (5N5) N_2 or Ar. The ion beam (spot size of approximately 2 mm, non-mass-selected, incident at mean angle of 55° to the surface normal) was rastered over the sample surface of approximately 8 mm × 8 mm. The typical accelerating voltage was 2.5 kV, in cases it varied between 1 and 5 kV. The current density measured at these settings changed in $(1–10) \times 10^{-6}$ A cm^{-2} range. At an energy of 2.5 keV, a characteristic (for the type of sample) steady state composition was achieved after about 15–30 min bombardment, corresponding to a fluence of $(1–5) \times 10^{17}$ ions cm^{-2}.

2.3. XPS analysis

XPS spectra were recorded on a Kratos XSAM 800 spectrometer operated in fixed retarding ratio or fixed analyzer transmission mode using Mg $K\alpha_{1,2}$ (1253.6 eV) or Al $K\alpha_{1,2}$ (1486.6 eV) excitation. The linearity of the energy scale was calibrated by the dual Al/Mg anode method, setting a 233.0-eV KE difference between the two Ag $3d_{5/2}$ lines. The pressure of the analysis chamber was lower than 10^{-7} Pa, which increased to approximately 5×10^{-5} Pa during ion bombardment. Wide-scan spectra in the 50–1250 eV kinetic energy range were recorded in 0.5-eV steps for all samples. Detailed spectra of the most intense core level lines of the constituent elements, the characteristic lines of the 'metal', the O 1s and N 1s, as well as of C 1s, the most common impurity, were recorded in 0.1-eV steps. At this applied resolution, the line energy positions could be determined with accuracy equal to or better than ±0.2 eV. Spectra were referenced to the C 1s line of the adventitious carbon set at 284.8 eV. The applicability of such referencing was proved using the gold decoration method by setting the Au $4f_{7/2}$ line to 84.0 eV. The complex line-shapes, developed after treatments, for the Ti 2p, V 2p, etc. doublets containing 3–4 discernibly shifted chemical states, were fitted with component peaks of constant half-widths and fixed energy separation of the doublets, allowing for the ½ components to be somewhat wider, taking into account the lifetime broadening [27]. Quantitative analysis, based on peak area intensity, was performed either with the Vision 2 or with the XPS MultiQuant program [28] using the experimentally determined photo-ionization cross-section data of Evans et al. [29] and the asymmetry parameters of Reilman et al. [30].

Following the described procedures in analysing the XP spectra, we could quantitatively evaluate the peak components of the reduced states. The results were justified by the self-consistency, e.g. by the correspondence of the measured overall oxygen content and the amount of oxygen required by the reduced metallic components, performed for the Ar ion bombarded SiO_2 and GeO_2 [31].

3. Results

3.1. Chemical state modifications caused by ion bombardment

It has been multiply reported that Ar^+ bombardment led to partial elimination of oxygen, i.e. reduction of oxides. Such process can be followed by XPS, primarily by detecting the change of the line-shape or the overall shift of the spectra of the metallic component. The other, in case not so easily detectable effect is the decrease of the oxygen to metal ratio, accessible sometime only by very accurately performed quantitative analysis. In this paragraph we will demonstrate these effects for the case of the N_2^+ bombardment, where, in addition to the reducing effect of the ion beam treatment, the amount and the chemical state of the built-in nitrogen is of a prime concern.

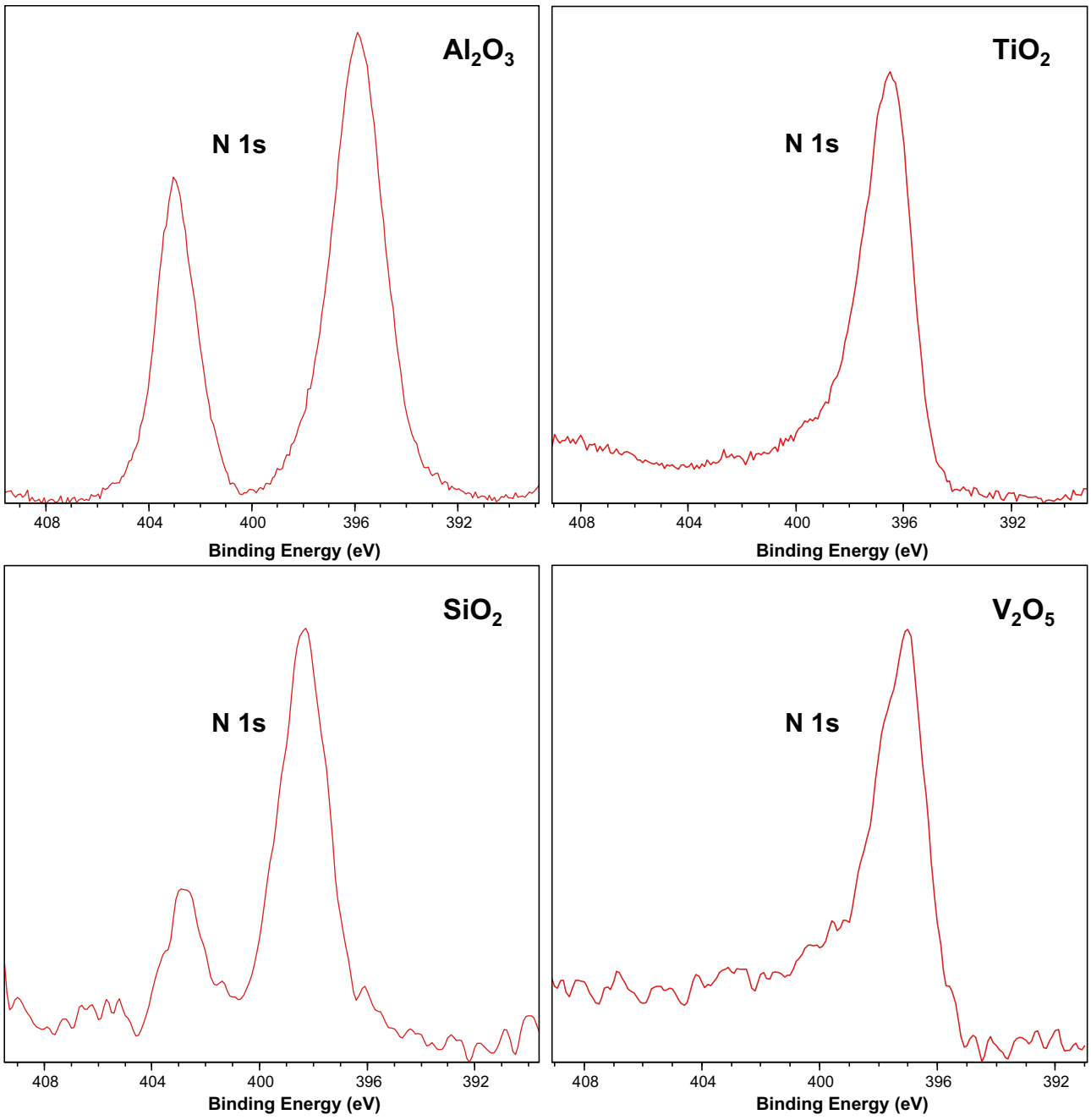

Fig. 1. The N 1s XP lines developed on the surface of Al_2O_3, SiO_2, TiO_2 and V_2O_5 after N_2^+ bombardment.

3.2. *Chemical state of the built-in nitrogen*

The chemical state of the nitrogen is characterized with confidence by the binding energy position of the N 1s line. The N 1s line recorded on chemically well defined nitride is of a simple Gaussian shape with a full width at half-height of approximately 1.6–1.9 eV. Any significant broadening is usually indicative of the presence of a new chemical state. The N 1s BE values fall in a relatively narrow energy range between 396 and 398 eV [32]. For the interstitial type nitrides like Ti, Zr, Hf, etc. the chemical shift is located in the lower BE range between 396 and 397 eV. The N 1s BE for more covalent nitrides of Si and Ge has values around 397 and 398 eV. The BE values for N–O bonds, i.e. for (NO), $–NO_2$ or $–NO_3$ groups are reported to be in the 403–408 eV energy range [33]. On this basis one can unambiguously define the chemical environment of the implanted nitrogen.

The N 1s lines of the implanted nitrogen for selected oxides are depicted in Fig. 1 and their BE is listed in Table 1. For comparison the N 1s BE for the corresponding nitrides and N–O compounds are also indicated in the table. As seen, the incorporated nitrogen forms bonds predominantly with the metal of the oxide judged by the similar chemical shift reported for the single-phase (stoichiometric) nitrides. In case of crystalline SiO_2, α-Al_2O_3, (and also of $MgAl_2O_4$ and GeO_2), a second type of nitrogen is also found with N 1s BE at about 403 eV [24], assignable to N in oxygen environment [33]. The origin and the nature of such nitrogen state will be discussed in the next paragraph. The asymmetry and low intensity features on the high BE side of the N 1s peak of TiO_2 and V_2O_5 are

Table 1
Position of the characteristic XPS lines for the metallic components of the oxides, the reduced states developed after Ar^+ and that of N 1s after N_2^+ bombardment.

Oxide	XPS line	Original state BE (eV)	Reduced states BE (eV)	N 1s implanted BE (eV)	N 1s in nitride BE (eV)	Chemical form [references]
Al_2O_3	Al 2p	73.6 (3^+)	72.4 (1^+)[a]	396.0	396.1	AlN [32,33,37]
				403.0	403.0	NO_2^- [33,34]
SiO_2	Si 2p	103.3 (4^+)	102.3 (3^+)	398.3	397.4	Si_3N_4 [32,37–42]
			101.2 (2^+)	402.9	403.0	(N_2) [42]
GeO_2	Ge $3d_{5/2}$	32.8 (4^+)	31.3 (2^+)	397.4	397.4	Ge_3N_4 [31,38,43]
ZrO_2	Zr $3d_{5/2}$	182.3 (4^+)	180.9 (2^+)	395.8	397.5	ZrN [25,32,46,48]
TiO_2	Ti $2p_{3/2}$	458.7 (4^+)	457.0 (3^+)	396.7	396.5	TiN [44–47]
			455.0 (2^+)			
V_2O_5	V $2p_{3/2}$	517.5 (5^+)	516.2 (4^+)	397.1	397.1	VN [25,49,50]
			515.1 (3^+)			
			514.1 (2^+)			
Nb_2O_5	Nb $3d_{5/2}$	207.3 (5^+)	205.7 (4^+)	397.0	397.0	NbN [25,51]
			204.0 (2^+)			

[a] Tentative assignment.

characteristic for this and some other transition metal nitrides and are related to various energy loss processes of the emerging photoelectrons in these compounds [27]. Formation of O–N–Me bonding configuration, for what the N 1s chemical shifts may fall in this intermediate 396–403 eV BE range, could not be excluded either.

3.3. Chemical state changes of the metals

The effect of the ion bombardment on the lineshape of the metallic components of some selected oxides is depicted in Figs. 2–4. While only minor changes, i.e. very small, ill-defined chemical shifts are detectable for Al_2O_3 and SiO_2 (Fig. 2), significant alterations are found for TiO_2 (Fig. 3) and V_2O_5 (Fig. 4). In the latter two cases the lineshape of the non-modified oxides and that of the Ar^+ bombarded states are also depicted for comparison. The obvious similarity of the lines of the two ion-bombarded states indicates that essentially similar reduced states are formed. Peak-fitting procedure was made including the minimum number of components. The results of the peak-synthesis procedure, the assignment of the peak-components and the identified chemical states for these two oxides are indicated in Figs. 3 and 4. Similar procedure was applied, or at least attempted, to the spectra of all modified oxides and the results are summarised in Table 1. The obtained data are in good agreement with the available reported values for the reduced oxides, nitrides and N-bonded states, e.g. for SiO_2, SiO_x, Si_3N_4, SiN_x in [32,33,37–42], for GeO_2, GeO_x in [31,38,43], for TiO_2, Ti_2O_3, TiO, TiN in [44–47], for ZrO_2 in [11,25,32,46,48], for V_2O_5, VO_2, V_2O_3, VN in [25,49,50] and for Nb_2O_5, NbN in [25,51].

3.4. Composition alterations

The change of the composition for the oxides as a consequence of the N_2^+ bombardment is listed in Table 2. For comparison the result of Ar^+ bombardment is also shown illustrating the entirely ballistic effect of the bombardment without the implications of the chemical effect of the nitrogen. The data represent the apparent steady state condition achievable at the applied experimental settings (ion energy, fluence-rate).

Two significantly different types of behaviour can be easily observed. There are oxides (Ge, Zr, Ti, V, Nb) that can be reduced

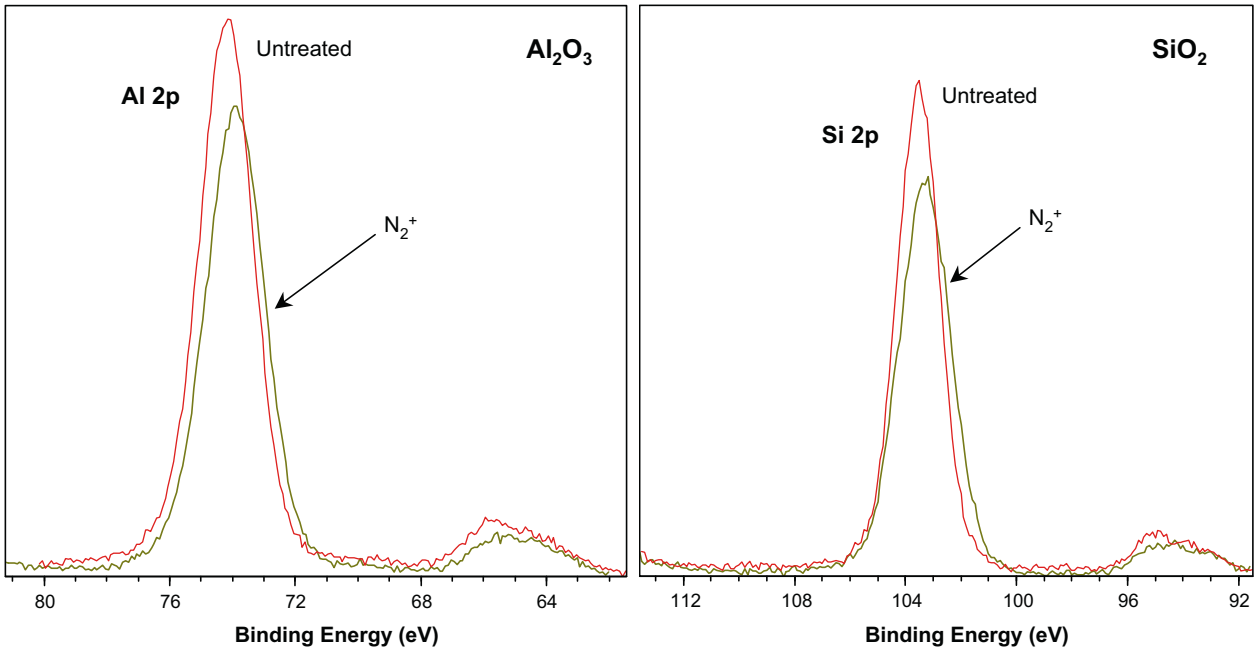

Fig. 2. The change of the Al 2p and Si 2p line-shape due to N_2^+ bombardment.

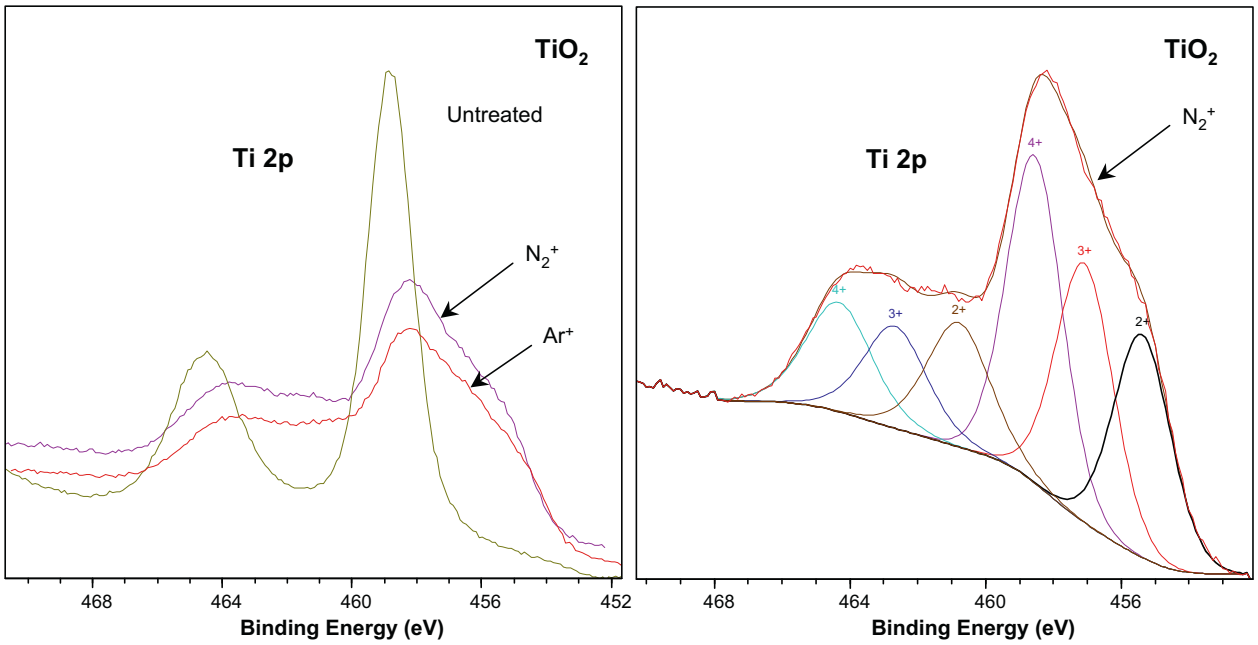

Fig. 3. The change of the Ti 2p line-shape due to N_2^+ and Ar^+ bombardment, and the result of the peak-synthesis, the oxidation states of titanium, developed at N_2^+ bombardment.

to a relatively large extent, incorporating high amount of nitrogen. Oxides of Al and Si seem to be less reducible and incorporating relatively lesser amount of nitrogen at similar bombardment conditions. In addition, only one part of the indicated N is bound to the metal, while the other is located in oxygen surrounding. In the last two columns in Table 2 the sampling depth of the O 1s XP line and the depth of modifications (range of penetration of the bombarding N ions) are listed for the oxides. It is known that 95% of the signal intensity originates from a depth of 3λ, where λ is the inelastic mean free pass of the O 1s electrons of 723 eV kinetic energy, calculated for the parent oxides according to [35]. The thickness of the modified depth by the N_2^+ ions of 2.5 keV energy (corresponding to 1.25 keV for each N ion) was calculated by the SRIM-2006 (Stopping and Range of Ions in Matter) program [36]. The results show that the thickness of the modified layer is somewhat greater, in most cases, than the sampling depth of the detected O 1s signal, and similarly to the N 1s signal, meaning that the measured intensities, i.e. the evaluated compositions are determined with adequate confidence, supposing relative homogeneity of the modified layer.

It is remarkable to point out the observed stability of the anion-to-cation ratio for most of the oxides irrespective of the type of bombardment, i.e. the constancy of the O/Me after Ar^+ and the (O + N)/Me after N_2^+ for these oxides.

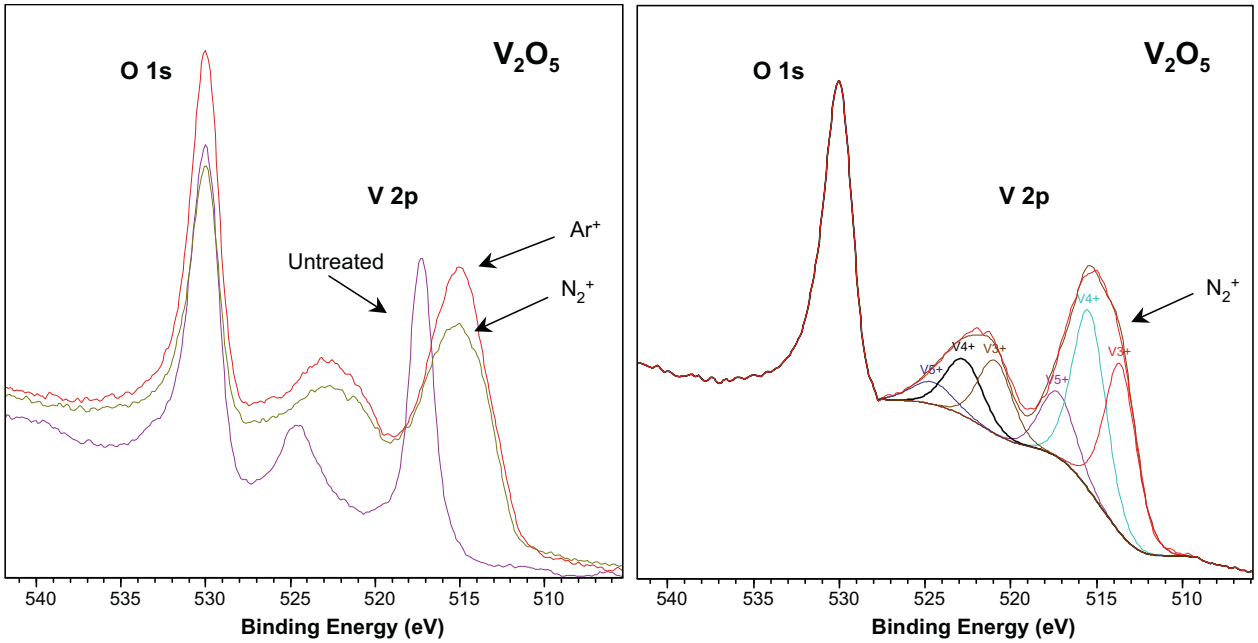

Fig. 4. The change of the V 2p line-shape and intensity change of the O 1s line due to N_2^+ and Ar^+ bombardment, and the result of the peak-synthesis of the V 2p doublet, and the oxidation states of vanadium, developed at N_2^+ bombardment.

Table 2
Surface composition of the oxides after Ar^+ and N_2^+ bombardment as derived from XPS peak areas, the relative amount (%) of O replaced by N, the sampling depth of the XPS measurement, equal to 3λ of the O 1s electrons at 720 eV KE [35], and thickness (*d*) of the modified layer, calculated for the penetration range of the 2.5 keV N_2^+ (1.25 keV N^+) ions in the different oxides by the SRIM program [36].

Oxide	Composition after bombardment			Sampling depth (3λ) (nm)	Ion range (*d*) (nm)
	Ar^+	N_2^+	O to N exchange (%)		
Al_2O_3 s.c.	$Al_2O_{2.7}$	$Al_2O_{2.4}N_{0.25}$[a]	8[a]	4.3	4.9
SiO_2 s.c.	$SiO_{1.8}$	$SiO_{1.7}N_{0.1}$[a]	7[a]	7.4	8.0
GeO_2 p.c.	$GeO_{1.4}$	$GeO_{1.3}N_{0.1}$	6	6.0	4.9
ZrO_2 s.c.	$ZrO_{1.6}$	$ZrO_{1.2}N_{0.4}$	20	4.6	6.0
TiO_2 s.c.	$TiO_{1.7}$	$TiO_{1.1}N_{0.6}$	30	4.8	5.4
V_2O_5 s.c.	$V_2O_{3.7}$	$V_2O_{2.7}N_{1.1}$	22	6.0	7.3
Nb_2O_5 p.c.	$Nb_2O_{3.6}$	$Nb_2O_{2.5}N_{1.2}$	24	5.8	7.0

s.c.: single crystalline; p.c.: poly-crystalline sample.
[a] Only one part of N bonded to Al or Si, the other is in O environment.

4. Discussion

The interaction of Ar^+ (and also other noble gas ions) with oxides leading to the development of reduced chemical states have been frequently reported [21–26]. The effect of energetic N ions or atoms on oxides is far less documented [37]. We have established a certain similarity of the two types of bombardment earlier [24–26,34]. Here we demonstrated the coexistence of the reduced oxidation states of the metal atoms with the nitride states leading to the obvious conclusion that not all the oxygen vacancies created by the nitrogen bombardment could be filled by nitrogen.

There are several questions to be answered in connection with the obtained results. One is the mechanism of the experimentally documented, although thermodynamically disfavoured reaction. Another one is the extent of the modification: the amount of oxygen lost and the amount of nitrogen built in. In connection with this the peculiar, most intriguing one-to-one atomic exchange of the excess loss of oxygen to nitrogen at nitrogen bombardment, compared to the oxygen loss at argon bombardment, and the observed stability of the anion-to-cation ratio irrespective of the type of bombardment.

4.1. Mechanism of oxygen replacement by nitrogen

The thermodynamic stability of the studied oxides is higher than the corresponding nitrides; at least, if we consider the stable highest oxidation states, i.e. replacement of O by N is disfavoured. In order to assess the feasibility of the observed oxygen loss and nitrogen incorporation, simplified hypotactic reactions of atomic N with the oxides were formulated and, for simplicity, the enthalpy changes (at 298 K) are collected in Table 3. The atomic state of N was considered here, in order to resemble the type of interaction taking place at nitrogen bombardment, where the bombarding N_2^+ ions dissociate when entering into the oxides. As seen, the enthalpy change for these reactions, normalised to one oxygen atom evolved, is positive for the high valence states, but may be negative for the lower valence oxides (TiO, VO, and NbO). It is important to note that high N/metal ratio (N/Me ∼0.6) is achieved for oxides having stable lower oxides. This fact not only shed light on the elementary processes taking place at ion bombardment, but also resolves the apparent conflict with the thermodynamic stabilities. As a consequence, a two-step process is proposed here: first oxygen vacancies, i.e. reduced states are created by the ballistic interactions, which will react, in the next step, by the implanted nitrogen atoms. The relatively high N/Me ∼0.4 ratio, measured for ZrO_2, is in contradiction with the very high positive ΔH, calculated for this reaction. This indicates that a lower oxidation state may exist also for zirconium. Although no thermochemical data was found for such a compound, crystallographic evidence of ZrO was reported [52], the existence of which will resolve this conflict.

4.2. The extent of oxygen replacement by nitrogen

The amount of oxygen replaced by nitrogen, given in Table 2, and included, as N/Me ratio, also in Table 3. Comparing these values to the calculated standard reaction enthalpies only some qualitative conclusions could be made. It is obvious, that the higher the stability of the parent oxide, and the more positive is the reaction enthalpy, the lower amount of nitrogen could be incorporated. The other, may be more important conclusion is, that, as discussed above, high oxygen to nitrogen exchange is achievable for those oxides where the metal has stable lower oxides. This again points out the primary role of the reduction, i.e. oxygen vacancy creation step preceding the accommodation of N.

Table 3
Standard enthalpy change of the hypothetical reactions of implanted N atoms with oxides and the measured nitrogen to metal ratios developed at steady states in N_2^+ bombardment, normalizedto one oxygen atom evolved.

Oxide	Reaction	$\Delta H_{298\,K}$ (eV/atom)	Measured N/Me
Al_2O_3	$Al_2O_3 + 2N(g) = 2AlN(s) + 3O(g)$	2.91	0.1[a]
SiO_2	$3SiO_2(s) + 4N(g) = Si_3N_4(s) + 6O(g)$	2.75	0.1[a]
GeO_2	$3GeO_2(s) + 4N(g) = Ge_3N_4(s) + 6O(g)$	2.06	0.1
ZrO_2	$ZrO_2(s) + N(g) = ZrN(s) + 2O$	3.95	0.4
TiO_2	$TiO_2(s) + N(g) = TiN(s) + 2O(g)$	3.28	0.6
TiO_2	$Ti_2O_3(s) + 2N(g) = 2TiN(s) + 3O(g)$	2.23	0.6
TiO_2	$TiO + N(g) = TiN(s) + O(g)$	−0.43	0.6
V_2O_5	$V_2O_5(s) + 2N(g) = 2VN(s) + 5O(g)$	2.94	0.55
V_2O_5	$V_2O_3(s) + 2N(g) = 2VN(s) + 3O(g)$	2.03	0.55
V_2O_5	$VO(s) + N(g) = VN(s) + O(g)$	−0.09	0.55
Nb_2O_5	$Nb_2O_5(s) + 2N(g) = 2NbN(s) + 5O(g)$	3.59	0.6
Nb_2O_5	$NbO(s) + N(g) = NbN(s) + O(g)$	−0.55	0.6

[a] Only one part of N bonded to Al or Si, the other is in O environment.

Finally we recall the similar anion:cation ratio at N_2^+ and at Ar^+ bombardment, meaning that a nitrogen atoms can be built-in into the oxide lattice, only if one 'excess' oxygen atom is removed from the partially reduced oxide at nitrogen beam treatment. On this basis we can deduce that existence of two neighbouring oxygen vacancies is the necessary precondition to the incorporation of a nitride type nitrogen atom, realising all three bonds with the neighbouring metal atoms.

4.3. The variable chemical environment of nitrogen

The specific feature of the presented ion-beam modification is that the implanted nitrogen is replacing the lattice oxygen atoms and incorporating by forming bonds to the metal atoms hosted in the oxide environment. This type of nitrogen is considered to be the building cluster of the oxinitride. In fact, only such type of N was proved to be catalytically active: e.g. photocatalytic activity of N-modified TiO_2 correlated with the concentration of the type of N with N 1s BE at 396 eV, contributing to the band gap narrowing of this oxide [1].

In certain oxides, e.g. in Al-, Si- and Ge-oxide, possessing strong directed O–Me bonds, part of the nitrogen is fixed in nitrite/nitrate-type form. Generation of such bonding states may be related rather to structure-directed, than to chemically preferred process, and can be interpreted as follows. It is known that e.g. in Al_2O_3 1/3 of the 'cation' sites are vacant, obviously, part of the implanted, but decelerated – in the collision cascade – low energy nitrogen atoms, unable to detach oxygen, may be trapped by filling these empty lattice sites surrounded entirely by oxygen atoms [34]. As a further support to this interpretation is that nitrate compounds are not form, but are inclined to decompose under ion bombardment [21], thus the observed appearance of N–O bonding is secured only by the structural peculiarity or by the oxygen-sublattice stability of the host oxide structure.

5. Conclusions

Surface of the transition metal oxides can be modified by N_2^+ ion bombardment of 1–5 keV energy creating by such treatment a few nanometre thick oxinitride layers.

The ballistic effect of the N_2^+ ion bombardment produces an oxygen deficient surface. The implanted nitrogen accommodates into the matrix of the partially reduced oxide by forming bonds predominantly with the metal, similar to those existing in the corresponding nitride.

Relatively large amount of nitrogen can be built into the oxides replacing 5–30% of the initially existing, stoichiometric lattice oxygen in the modified surface layer.

High level of N-incorporation was observed for thermodynamically less stable oxides, having lower valence state oxides.

XPS proved to be adequate tool for the complex evaluation of these modification processes, by providing reliable data for the establishing the interactions among the components, the chemical structure of the resulting surface and for the quantitative assessment of the modification.

Acknowledgements

The author is indebted to M. Mohai for his valuable contribution of the quantitative evaluation of the data by the MultiQuant program and also to L. Gulyás for technical assistance.

References

[1] R. Asahi, T. Morikawa, T. Ohwaki, K. Aoki, Y. Taga, Science 293 (2001) 269.
[2] C. Zhang, A. Michaelides, D.A. King, S.J. Jenkins, J. Am. Chem. Soc. 132 (2010) 2175.
[3] C. Wang, L. Yin, L. Zhang, D. Xiang, R. Gao, Sensors 10 (2010) 2088.
[4] F.E. Osterloh, Chem. Mater. 20 (2008) 35.
[5] D. Logvinovich, Anionic substitution in perovskite-type oxides, Thesis, Augsburg University, 2008.
[6] L. Le Gendre, R. Marchand, Y. Laurent, J. Eur. Ceram. Soc. 17 (1997) 1813.
[7] L. Le Gendre, R. Marchand, B. Piriou, Eur. J. Solid State Inorg. Chem. 34 (1997) 973.
[8] R. Marchand, Y. Laurent, J. Guyader, P. L'Haridon, P. Verdier, J. Eur. Ceram. Soc. 8 (1991) 197.
[9] R. Marchand, F. Tessier, A. Le Sauze, N. Diot, Int. J. Inorg. Mater. 3 (2001) 1143.
[10] Y.-I. Kim, P.M. Woodward, K.Z. Baba-Kishi, C.W. Tai, Chem. Mater. 16 (2004) 1267.
[11] H. Soerijanto, C. Rödel, U. Wild, M. Lerch, R. Schomäcker, R. Schlögl, T. Ressler, J. Catal. 250 (2007) 19.
[12] T. Otremba, N. Frenzel, M. Lerch, T. Ressler, R. Schomäcker, Appl. Catal. A: Gen. 392 (2011) 103.
[13] V. Bharat, R. Boppana, D.J. Doren, R.F. Lobo, Chem. Sus. Chem. 3 (2010) 814.
[14] J. Huang, Y. Cui, X. Wang, Environ. Sci. Technol. 44 (2010) 3500.
[15] R. Marchand, R. Conanec, Y. Laurent, Ph. Bastians, P. Grange, L.M. Gandia, M. Montes, J. Fernandes, Appl. Catal. A: Gen. 114 (1994) L191.
[16] N. Fripiat, R. Conanec, R. Marchand, Y. Laurent, P. Grange, J. Eur. Ceram. Soc. 17 (1997) 2011.
[17] P. Wu, R. Xie, J.A. Imlay, J.Ku. Shang, Appl. Catal. B: Environ. 88 (2009) 576.
[18] C.-C. Hu, H. Teng, J. Phys. Chem. C 114 (2010) 20100.
[19] R. Abe, M. Higashi, K. Domen, J. Am. Chem. Soc. 132 (2010) 11828.
[20] K. Maeda, K. Domen, J. Phys. Chem. C 111 (2007) 78517861.
[21] G. Betz, G.K. Wehner, in: R. Behrisch (Ed.), Topics in Applied Physics, vol. 52, Springer, Berlin, 1983, p. 11 (and references cited therein).
[22] S. Hofmann, J.M. Sanz, J. Trace Microprobe Tech. 1 (1982–1983) 213.
[23] J.L. Sullivan, S.O. Saied, I. Bertóti, Vacuum 42 (1991) 1203.
[24] I. Bertóti, R. Kelly, M. Mohai, A. Tóth, Surf. Interface Anal. 19 (1992) 291.
[25] I. Bertóti, R. Kelly, M. Mohai, A. Tóth, Nucl. Instr. Methods B 80/81 (1993) 1219.
[26] R. Kelly, I. Bertóti, A. Miotello, Nucl. Instr. Methods B 80/81 (1993) 1154.
[27] D. Briggs, J.C. Riviére, in: D. Briggs, M.P. Seah (Eds.), Practical Surface Analysis, John Wiley & Sons, Inc., New York, 1990, p. 85 (Chapter 3).
[28] M. Mohai, Surf. Interface Anal. 36 (2004) 828, doi:10.1002/sia.1775.
[29] S. Evans, R.G. Pritchard, J.M. Thomas, J. Electron Spectrosc. Relat. Phenom. 14 (1978) 341.
[30] R.F. Reilman, A. Msezane, S.T. Mansor, J. Electron Spectrosc. Relat. Phenom. 8 (1976) 389.
[31] I. Bertóti, M. Menyhard, A. Tóth, in: J.C. Riviére, S. Myhra (Eds.), Handbook of Surface and Interface Analysis: Methods for Problem-solving, Marcel Decker, Inc., New York, 1998, pp. 297–346.
[32] I. Bertoti, Surf. Coat. Technol. 151–152 (2002) 194.
[33] C.D. Wagner, W.M. Riggs, L.E. Davis, J.F. Moulder, G.E. Muilenberg:, Handbook of X-ray Photoelectron Spectroscopy , Physical Electronics Division, Perkin-Elmer Corporation, Eden Prairie, Minnesota, 1979.
[34] J.P. Espinós, A.R. González-Elipe, M. Mohai, I. Bertóti, Surf. Interface Anal. 30 (2000) 90.
[35] W.H. Gries, Surf. Interface Anal. 24 (1996) 38.
[36] J.F. Ziegler, J.P. Biersack, M.D. Ziegler, SRIM 2006:The Stopping and Range of Ions in Matter. http://www.srim.org/#SRIM.
[37] J.A. Taylor, J.W. Rabalais, J. Chem. Phys. 75 (1981) 1735.
[38] J.A. Taylor, G.M. Lancaster, J.W. Rabalais:, J. Electron Spectrosc. Relat. Phenom. 13 (1978) 435.
[39] J.F. Moulder, W.F. Stickle, P.E. Sobol, K.D. Bomben, Handbook of X-ray Photoelectron Spectroscopy , Physical Electronics Division, Perkin-Elmer Corporation, Eden Prairie, Minnesota, 1992.
[40] F. Pavlyák, I. Bertóti, M. Mohai, I. Biczó, J. Giber, Surf. Interface Anal. 20 (1993) 221.
[41] O. Benkherourou, J.P. Deville, J. Vac. Sci. Technol. A 6 (1988) 3125.
[42] H. Jin, S.K. Oh, H.J. Kang, J.C. Lee, J. Korean Phys. Soc. 51 (2007) 1042.
[43] Y. Takano, Y. Tandoh, H. Ozaki, N. Mori, Phys. Status Solidi (b) 130 (1985) 431.
[44] I. Bertóti, M. Mohai, J.L. Sullivan, S.O. Saied, Surf. Interface Anal. 21 (1994) 467.
[45] I. Bertóti, M. Mohai, J.L. Sullivan, S.O. Saied, Appl. Surf. Sci. 84 (1995) 357.
[46] H. Höchst, R.D. Bringans, P. Steiner, Th. Wolf, Phys. Rev. B 25 (1982) 7183.
[47] L. Bugyi, A. Berkó, L. Óvári, A.M. Kiss, J. Kiss, Surf. Sci. 602 (2008) 1650.
[48] S. Badrinarayanan, S. Sinha, A.B. Mandale, J. Electron Spectrosc. Relat. Phenom. 49 (1989) 303.
[49] M. Demeter, M. Neuman, W. Reichelt, Surf. Sci. 454–456 (2000) 41.
[50] Y.M. Shulg1'ga, V.N. Troitskii, M.I. Aivazov, Y.G. Borodk'o, Zh. Neorg. Khim. 21 (1976) 2621.
[51] M.K. Bahl, J. Phys. Chem. Solids 36 (1975) 485.
[52] X. Zhe, A. Hendry, J. Mater. Sci. Lett. 17 (1998) 687.